

Neutrino spin oscillations in a magnetized Polish doughnut

Maxim Dvornikov

Pushkov Institute of Terrestrial Magnetism, Ionosphere and Radiowave Propagation (IZMIRAN), 108840 Moscow, Troitsk, Russia

E-mail: maxdvo@izmiran.ru

Abstract. We study the gravitational scattering of ultrarelativistic neutrinos off a rotating supermassive black hole (BH) surrounded by a thick magnetized accretion disk. Neutrinos interact electroweakly with background matter and with the magnetic field in the disk since neutrinos are supposed to possess nonzero magnetic moments. The interaction with external fields results in neutrino spin oscillations. We find that the toroidal magnetic field, inherent in the magnetized Polish doughnut, does not cause a significant spin-flip for any reasonable strengths of the toroidal component. The reduction of the observed neutrino flux, owing to neutrino spin oscillations, is predicted. A poloidal component of the magnetic field gives the main contribution to the modification of the observed flux. The neutrino interaction with matter, rotating with relativistic velocities, also changes the flux of neutrinos. We briefly discuss the idea of the neutrino tomography of magnetic field distributions in accretion disks near BHs.

Keywords: neutrino properties, astrophysical black holes, magnetic fields, accretion

ArXiv ePrint: [2307.10126](https://arxiv.org/abs/2307.10126)

Contents

1	Introduction	1
2	Neutrino scattering off a rotating BH	2
3	Neutrino spin evolution in curved spacetime under the influence of external fields	3
4	External fields in an accretion disk	5
5	Parameters of the system	6
6	Results	7
7	Conclusion	10
A	Magnetized Polish doughnut accounting for the poloidal magnetic field	11
B	Solution of the Schrödinger equation for neutrinos below the equatorial plane	14

1 Introduction

The experimental achievements, e.g., in refs. [1, 2], confirmed that neutrinos are massive particles and there is a nonzero mixing between different neutrino generations. These results open a window to explore physics beyond the standard model. The nonzero neutrino masses inevitably result in nontrivial neutrino electromagnetic properties. Namely, it is shown in refs. [3, 4] that, even in the minimally extended standard model supplied with a right handed neutrino, there is a small neutrino magnetic moment. It means that a neutrino is no longer considered as a purely electrically neutral particle. For example, a nonzero neutrino magnetic moment leads to the particle spin precession in an external magnetic field.

The change of the neutrino polarization in external fields has dramatic consequences for the observability of these particles. In frames of the standard model, a neutrino is created as a left-handed particle, i.e. its spin is opposite to the neutrino momentum. If the neutrino polarization changes, the particle becomes right-handed, i.e. sterile. Hence, we shall observe the effective reduction of the initial neutrino flux. This process is called neutrino spin oscillations. Spin oscillations of astrophysical neutrinos were thoroughly studied by many authors (see, e.g., ref. [5]). For example, the upper bound on the neutrino magnetic moment by studying spin oscillations of supernova (SN) neutrinos was obtained in ref. [6].

It was demonstrated in ref. [7] that, besides the interaction with a magnetic field, neutrino spin oscillations can be affected by the neutrino electroweak interaction with background matter. The gravitational interaction, although it is quite weak, can also cause the precession of a fermion spin. It was shown in ref. [8] that the motion of a spinning body in a curved spacetime deviates from geodesic. Assuming that a fermion is an elementary particle, it was obtained in ref. [9] that its spin is parallel transported along the particle trajectory. The quantum theory of the fermion spin in curved spacetime was developed in ref. [10].

Using the quasiclassical approach in ref. [9], neutrino spin oscillations in curved spacetime were studied in ref. [11] within the General Relativity (GR), and its extensions in refs. [12–15]. In this work, we continue the studies in refs. [16–18], where spin effects in the neutrino gravitational scattering off a rotating black hole (BH) are accounted for. In a gravitational scattering, both incoming and outgoing neutrinos are in the asymptotically flat spacetime. Therefore, their spin states are well defined.

As shown in refs. [16–18], the magnetic field in an accretion disk gives the main contribution to neutrino spin oscillations. However, we used quite simple models of accretion disk in those papers. It should be noted that an accretion disk should be thick in order that both magnetic field and background matter are able to influence neutrino spin oscillations.

In the present work, we rely on the thick accretion disk model call a Polish doughnut [19]. The magnetized version of a Polish doughnut was developed in ref. [20]. We also account for the possibility of the presence of a poloidal magnetic field inside the accretion disk. One of the models for such a field was proposed in ref. [21]. Other models of accretion disks are reviewed in ref. [22].

The present work was motivated by the recent observations of the BH shadows in the centers of M87 and our Galaxy in refs. [23, 24]. It is the first direct test of GR in the strong field limit. It was suggested in ref. [25] that, besides photons emitted by an accretion disk, it can be a source of high energy neutrinos. It should be noted that there are active searches for high energy neutrinos emitted in active galactic nuclei, e.g., in ref. [26].

The image of such a disk, observed in a neutrino telescope, should account for both strong gravitational lensing of particles, as well as the neutrino spin precession in external fields, which converts active left neutrinos to sterile ones. Thus, in a neutrino telescope, we shall observe a different picture compared to an optical image plotted, e.g., in ref. [27]. Another possibility to probe spin effects in the neutrino gravitational scattering is to observe the lensing of SN neutrinos by a supermassive BH (SMBH) in the center of our Galaxy. For example, such a possibility was discussed in ref. [28].

Our work is organized as follows. We recall how to describe the trajectory of ultrarelativistic particles scattered off a rotating BH in section 2. In section 3, we represent the neutrino spin evolution in external fields in curved spacetime. The structure of external fields in the accretion disk is given in section 4. We fix the characteristics of the external fields and a neutrino in section 5. In section 6, we present the results of numerical simulations. Finally, we conclude in section 7. The main expressions for a magnetized Polish doughnut are listed in appendix A. In appendix B, we show how to use the symmetry of the system to reconstruct the spin precession of some neutrinos.

2 Neutrino scattering off a rotating BH

In this section, we briefly remind how to describe the motion of ultrarelativistic neutrinos scattered off a rotating BH.

The spacetime of a rotating BH has the Kerr metric which is written down in the following form using the Boyer-Lindquist coordinates $x^\mu = (t, r, \theta, \phi)$:

$$ds^2 = g_{\mu\nu} dx^\mu dx^\nu = \left(1 - \frac{rr_g}{\Sigma}\right) dt^2 + 2\frac{rr_g a \sin^2 \theta}{\Sigma} dt d\phi - \frac{\Sigma}{\Delta} dr^2 - \Sigma d\theta^2 - \frac{\Xi}{\Sigma} \sin^2 \theta d\phi^2, \quad (2.1)$$

where

$$\Delta = r^2 - rr_g + a^2, \quad \Sigma = r^2 + a^2 \cos^2 \theta, \quad \Xi = (r^2 + a^2) \Sigma + rr_g a^2 \sin^2 \theta. \quad (2.2)$$

Here r_g is the Schwarzschild radius. The mass of BH is $M = r_g/2$ and its spin, which is along the z -axis, is $J = Ma$, where $0 < a < M$.

The motion of a test ultrarelativistic particle in the metric in eq. (2.1) can be found in quadratures [29]. It has three integrals of motion: the particle energy, E , its angular momentum, L , and the Carter constant, Q . In the scattering problem, $Q > 0$. It was shown in ref. [30] that form of the trajectory can be inferred from the integral expressions,

$$z \int \frac{dx}{\pm\sqrt{R(x)}} = \int \frac{dt}{\pm\sqrt{\Theta(t)}}, \quad (2.3)$$

$$\phi = z \int \frac{(x - zy)dx}{\pm\sqrt{R(x)}(x^2 - x + z^2)} + \frac{y}{z} \int \frac{dt}{\pm\sqrt{\Theta(t)}(1 - t^2)} \quad (2.4)$$

where

$$\begin{aligned} R(x) &= (x^2 + z^2 - yz)^2 - (x^2 - x + z^2) [w + (z - y)^2], \\ \Theta(t) &= (t_-^2 + t^2)(t_+^2 - t^2), \\ t_{\pm}^2 &= \frac{1}{2z^2} \left[\sqrt{(z^2 - y^2 - w)^2 + 4z^2w} \pm (z^2 - y^2 - w) \right], \end{aligned} \quad (2.5)$$

We use the dimensionless variables in eqs. (2.3)-(2.5): $x = r/r_g$, $y = L/r_g E$, $z = a/r_g$, $w = Q/r_g^2 E^2$, and $t = \cos \theta$.

The strategy for finding the neutrino trajectory is the following. First, one computes the x -integral in eq. (2.3) numerically. Then, $\theta = \arccos t$ is obtained from eq. (2.3) using the Jacobi elliptic functions. At this stage, we should account for inversions of the trajectory in the equatorial plane. Finally, eq. (2.4) is used to get ϕ . The details of calculations are provided in ref. [31].

3 Neutrino spin evolution in curved spacetime under the influence of external fields

In this section, we consider the description of the neutrino polarization when a particle scatters off a rotating BH surrounded by a realistic thick magnetized accretion disk.

The covariant four vector of the spin S^μ of a neutrino, which interacts with an electromagnetic field and background matter, obeys the following equation in curved spacetime [32],

$$\frac{DS^\mu}{d\tau} = 2\mu \left(F^{\mu\nu} S_\nu - U^\mu U_\nu F^{\nu\lambda} S_\lambda \right) + \sqrt{2} G_F E^{\mu\nu\lambda\rho} G_\nu U_\lambda S_\rho, \quad (3.1)$$

where $DS^\mu = dS^\mu + \Gamma_{\alpha\beta}^\mu S^\alpha dx^\beta$ is the covariant differential, $\Gamma_{\alpha\beta}^\mu$ are the Christoffel symbols, $U^\mu = \frac{dx^\mu}{d\tau}$ is the neutrino four velocity in the world coordinates, τ is the proper time, $E^{\mu\nu\lambda\rho} = \frac{1}{\sqrt{-g}} \varepsilon^{\mu\nu\lambda\rho}$ is the covariant antisymmetric tensor in a curved spacetime, $g = \det(g_{\mu\nu})$ is the determinant of the metric tensor, $F_{\mu\nu}$ is the tensor of an external electromagnetic field, μ is the neutrino magnetic moment, $G_F = 1.17 \times 10^{-5} \text{ GeV}^{-2}$ is the Fermi constant, and G_μ is the covariant effective potential of the neutrino electroweak interaction with a background matter. Equation (3.1) is valid for both massive and massless (ultrarelativistic) neutrinos.

The neutrino polarization is defined in the locally Minkowskian frame $x_a = e_a^\mu x_\mu$. The vierbein vectors e_a^μ satisfy the relation, $\eta_{ab} = e_a^\mu e_b^\nu g_{\mu\nu}$, where $\eta_{ab} = (1, -1, -1, -1)$ is the

Minkowski metric tensor. One can check that e_a^μ have the form,

$$\begin{aligned} e_0^\mu &= \left(\sqrt{\frac{\Xi}{\Sigma\Delta}}, 0, 0, \frac{arr_g}{\sqrt{\Delta\Sigma\Xi}} \right), & e_1^\mu &= \left(0, \sqrt{\frac{\Delta}{\Sigma}}, 0, 0 \right), \\ e_2^\mu &= \left(0, 0, \frac{1}{\sqrt{\Sigma}}, 0 \right), & e_3^\mu &= \left(0, 0, 0, \frac{1}{\sin\theta} \sqrt{\frac{\Sigma}{\Xi}} \right), \end{aligned} \quad (3.2)$$

where Δ , Σ , and Ξ are given in eq. (2.2).

We rewrite eq. (3.1) in this Minkowskian frame making the boost to the particle rest frame, where the invariant three vector of the neutrino polarization, ζ , is defined,

$$\frac{d\zeta}{dt} = 2(\zeta \times \Omega). \quad (3.3)$$

The vector $\Omega = \Omega_g + \Omega_{\text{em}} + \Omega_{\text{matt}}$, which incorporates the neutrino interaction with external fields including gravity, has the following form for an ultrarelativistic neutrino:

$$\begin{aligned} \Omega_g &= \frac{1}{2Ut} \left[\mathbf{b}_g + \frac{1}{1+u^0} (\mathbf{e}_g \times \mathbf{u}) \right], \\ \Omega_{\text{em}} &= \frac{\mu}{Ut} \left[u^0 \mathbf{b} - \frac{\mathbf{u}(\mathbf{u}\mathbf{b})}{1+u^0} + (\mathbf{e} \times \mathbf{u}) \right], \\ \Omega_{\text{matt}} &= \frac{G_F \mathbf{u}}{\sqrt{2}Ut} \left(g^0 - \frac{(\mathbf{g}\mathbf{u})}{1+u^0} \right), \end{aligned} \quad (3.4)$$

where $(\mathbf{e}_g, \mathbf{b}_g) = G_{ab} = \gamma_{abc} u^c$, $\gamma_{abc} = \eta_{ad} e_{\mu;\nu}^d e_b^\mu e_c^\nu$ are the Ricci rotation coefficients, the semicolon stays for the covariant derivative, $(\mathbf{e}, \mathbf{b}) = f_{ab} = e_a^\mu e_b^\nu F_{\mu\nu}$ is the electromagnetic field tensor in the locally Minkowskian frame, $(u^0, \mathbf{u}) = u^a = e_a^\mu U^\mu$, and $(g^0, \mathbf{g}) = g^a = e_a^\mu G^\mu$.

The electric and magnetic fields are $e_i = f_{0i}$ and $b_i = -\varepsilon_{ijk} f_{jk}$, where ε_{ijk} is the antisymmetric tensor in the flat spacetime. The explicit form of these vectors depends on the original configuration of the electromagnetic field in world coordinates $F_{\mu\nu}(x^\mu)$. These vectors for certain models of electromagnetic fields in an accretion disk versus r and θ are given shortly in section 4; cf. eqs. (4.3)-(4.5).

Instead of solving the precession eq. (3.3), we deal with the effective Schrödinger equation to describe the neutrino polarization,

$$i \frac{d\psi}{dx} = \hat{H}_x \psi, \quad \hat{H}_x = -\mathcal{U}_2 (\boldsymbol{\sigma} \cdot \boldsymbol{\Omega}_x) \mathcal{U}_2^\dagger, \quad (3.5)$$

where $\boldsymbol{\sigma} = (\sigma_1, \sigma_2, \sigma_3)$ are the Pauli matrices, $\boldsymbol{\Omega}_x = r_g \boldsymbol{\Omega} \frac{dt}{dr}$, and $\mathcal{U}_2 = \exp(i\pi\sigma_2/4)$. Equation (3.5) is rewritten in dimensionless variables and adapted for the scattering problem. It is convenient to rewrite the vector $\boldsymbol{\Omega}_x$ in the form,

$$\begin{aligned} \boldsymbol{\Omega}_x^{(g)} &= \frac{1}{2} \left[\tilde{\mathbf{b}}_g + (\tilde{\mathbf{e}}_g \times \mathbf{v}) \right], \\ \boldsymbol{\Omega}_x^{(\text{em})} &= V_B \left[l^0 \mathbf{b} - \mathbf{v}(\mathbf{l}\mathbf{b}) + (\mathbf{e} \times \mathbf{l}) \right], \\ \boldsymbol{\Omega}_x^{(\text{matt})} &= V_m \mathbf{l} \left[g^0 - (\mathbf{g}\mathbf{v}) \right], \end{aligned} \quad (3.6)$$

where the vectors $(l^0, \mathbf{l}) = l^a = \frac{dt}{dr} \frac{u^a}{U^t}$, $\mathbf{v} = \frac{\mathbf{u}}{1+u^0}$, $\tilde{\mathbf{e}}_g = \mathbf{e}_g \frac{r_g}{U^t} \frac{dt}{dr}$ and $\tilde{\mathbf{b}}_g = \mathbf{b}_g \frac{r_g}{U^t} \frac{dt}{dr}$, are finite for an ultrarelativistic neutrino. Note that $\tilde{\mathbf{e}}_g$ and $\tilde{\mathbf{b}}_g$ are the linear functions of $\frac{dx^\mu}{dr}$ which

can be calculated using the results of section 2. The explicit form of l^a and \mathbf{v} is provided in ref. [16].

The scalar quantity V_B depends on the configuration of the magnetic field in the disk, which is discussed shortly in section 4. The parameter $V_m = \frac{G_F \rho}{\sqrt{2} m_p r_g}$ for a hydrogen plasma, where ρ is the mass density of the disk and m_p is the proton mass.

The effective spinor ψ in eq. (3.5) has form $\psi_{-\infty}^T = (1, 0)$ for incoming neutrinos. Such a spinor corresponds to a left polarized active neutrino. For a scattered particle, after solving eq. (3.5) along the neutrino trajectory, it becomes $\psi_{+\infty}^T = (\psi_{+\infty}^{(R)}, \psi_{+\infty}^{(L)})$. The survival probability, i.e. the probability that a neutrino remains left polarized in the wake of the scattering, is $P_{LL} = |\psi_{+\infty}^{(L)}|^2$.

4 External fields in an accretion disk

In this section, we discuss the properties of the background matter and the magnetic fields in an accretion disk which a neutrino interacts with.

We treat electroweak interaction of a neutrino with background fermions in the forward scattering approximation. We mention in section 3 that this interaction is characterized by the four potential G^μ , which has the following form in the hydrogen plasma:

$$G^\mu = \sum_{f=e,p} q_f J_f^\mu, \quad (4.1)$$

where $J_f^\mu = n_f U_f^\mu$ are the hydrodynamic currents, n_f are the invariant fermions densities, U_f^μ are their four velocities in the disk, and q_f are the constants which are found in the explicit form in ref. [33]. We suppose in eq. (4.1) that matter is unpolarized. We take that $n_e = n_p$ because of the plasma electroneutrality and $U_e^\mu = U_p^\mu$, i.e. there is no differential rotation between the components of plasma.

In the model of a Polish doughnut, one has that $U_f^\mu = (U_f^t, 0, 0, U_f^\phi)$; cf. eq. (A.2). Thus, using eq. (3.2), we get that the nonzero components of g^a in eq. (3.6) are

$$g^0 = \frac{\sqrt{x^2 + z^2 \cos^2 \theta} \sqrt{x^2 - x + z^2} U_f^t}{\sqrt{z^2 \cos^2 \theta (x^2 - x + z^2) + z^2 x^2 + z^2 x + x^4}},$$

$$g^3 = \frac{\sin \theta \left[r_g U_f^\phi (z^2 \cos^2 \theta (x^2 - x + z^2) + z^2 x^2 + z^2 x + x^4) - U_f^t x z \right]}{\sqrt{x^2 + z^2 \cos^2 \theta} \sqrt{z^2 \cos^2 \theta (x^2 - x + z^2) + z^2 x^2 + z^2 x + x^4}}. \quad (4.2)$$

The mass density ρ , which enters in the coefficient V_m , is given in eq. (A.4).

Now, we discuss the neutrino interaction with magnetic fields. The toroidal magnetic is inherent in the magnetized Polish doughnut model. The four vector of such a magnetic field is $B^\mu = (B^t, 0, 0, B^\phi)$; cf. eq. (A.2). The electromagnetic field tensor of this field has the only nonzero components $F^{r\theta} = -F^{\theta r}$. Based on eq. (3.2), we get that the nonzero component of \mathbf{b} in eq. (3.6) is

$$b_3 = - \frac{U_f^t r_g^2 \sqrt{2 p_m^{(\text{tor})}}}{\sin \theta (1 - \Omega l_0) \sqrt{(x^2 + z^2 \cos^2 \theta)(x^2 - x + z^2)}} \times \left\{ \lambda_0^2 (x^2 - x + z^2 \cos^2 \theta) + 2 \lambda_0 x z \sin^2 \theta - \sin^2 \theta [(x^2 + z^2)(x^2 + z^2 \cos^2 \theta) + x z^2 \sin^2 \theta] \right\}^{1/2}, \quad (4.3)$$

where $\lambda_0 = l_0/r_g$, l_0 is the constant angular momentum in the disk (see appendix A), Ω is given in eq. (A.3), and $p_m^{(\text{tor})}$ is the magnetic pressure of the toroidal field present in eq. (A.4). The vector $\mathbf{e} = 0$. The dimensionless coefficient V_B in eq. (3.6) is $V_B = \mu/r_g$.

A poloidal magnetic field is not a part of the magnetized Polish doughnut model. It is, however, known that a superposition of poloidal and toroidal components makes the resulting magnetic field more stable. That is why we include a poloidal field in our calculations. We consider two models for a poloidal field.

First, we take a field which asymptotically tends to a constant one parallel to the rotation axis of BH at the infinity. The vector potential for such a field is given in eq. (A.7). The nonzero components of the dimensionless vectors \mathbf{e} and \mathbf{b} are

$$\begin{aligned}
e_1 &= f_B(x) \frac{z [z^2 \cos^4 \theta (z^2 - x^2) + \cos^2 \theta (z^4 + 2z^2 x^2 - 3x^4) - z^2 x^2 + x^4]}{2\sqrt{z^2 \cos^2 \theta (x^2 - x + z^2) + z^2 x^2 + z^2 x + x^4 (x^2 + z^2 \cos^2 \theta)^2}}, \\
e_2 &= \frac{f_B(x) x z^3 \sin 2\theta \sqrt{x^2 - x + z^2} (1 + \cos^2 \theta)}{2\sqrt{z^2 \cos^2 \theta (x^2 - x + z^2) + z^2 x^2 + z^2 x + x^4 (x^2 + z^2 \cos^2 \theta)^2}}, \\
b_1 &= \frac{f_B(x) \cos \theta [(x^2 + z^2 \cos^2 \theta)^2 (x^2 - x + z^2) + x(x^4 - z^4)]}{\sqrt{z^2 \cos^2 \theta (x^2 - x + z^2) + z^2 x^2 + z^2 x + x^4 (x^2 + z^2 \cos^2 \theta)^2}}, \\
b_2 &= f_B(x) \sin \theta \sqrt{x^2 - x + z^2} \\
&\quad \times \frac{[z^4 \cos^4 \theta (1 - 2x) + z^2 \cos^2 \theta (z^2 - x^2 - 4x^3) - z^2 x^2 - 2x^5]}{2\sqrt{z^2 \cos^2 \theta (x^2 - x + z^2) + z^2 x^2 + z^2 x + x^4 (x^2 + z^2 \cos^2 \theta)^2}}, \tag{4.4}
\end{aligned}$$

where, following ref. [34], we introduce the additional factor $f_B(x) = x^{-5/4}$ to provide the scaling of the magnetic field with the distance $B \propto r^{-5/4}$. The dimensionless coefficient V_B in eq. (3.6), corresponding to such a field, is $V_B = \mu B_0 r_g$, where B_0 is the magnetic field strength near BH at $x \sim 1$.

Second, we consider a poloidal field generated by the vector potential in eq. (A.8). In this case, the nonzero components of vectors \mathbf{e} and \mathbf{b} in eq. (3.6) are

$$\begin{aligned}
e_1 &= - \frac{z x b r_g \partial_r \rho}{(x^2 + z^2 \cos^2 \theta) \sqrt{z^2 \cos^2 \theta (x^2 - x + z^2) + z^2 x^2 + z^2 x + x^4}}, \\
e_2 &= - \frac{z x b \partial_\theta \rho}{(x^2 + z^2 \cos^2 \theta) \sqrt{x^2 - x + z^2} \sqrt{z^2 \cos^2 \theta (x^2 - x + z^2) + z^2 x^2 + z^2 x + x^4}}, \\
b_1 &= - \frac{b \partial_\theta \rho}{\sin \theta \sqrt{z^2 \cos^2 \theta (x^2 - x + z^2) + z^2 x^2 + z^2 x + x^4}}, \\
b_2 &= \frac{\sqrt{x^2 - x + z^2} b r_g \partial_r \rho}{\sin \theta \sqrt{z^2 \cos^2 \theta (x^2 - x + z^2) + z^2 x^2 + z^2 x + x^4}}, \tag{4.5}
\end{aligned}$$

where ρ and b are given in eqs. (A.4) and (A.8). The density derivatives with respect to r and θ can be calculated analytically using eq. (A.4). However, the corresponding expressions are quite cumbersome and, thus, we omit them. The dimensionless coefficient V_B in eq. (3.6) is $V_B = \mu/r_g$ for this field component.

5 Parameters of the system

In this section, we specify the values of the parameters of a neutrino and external fields, as well as describe some details of calculations.

We suppose that a neutrino is a Dirac particle possessing a nonzero magnetic moment μ . Its value is $\mu = 10^{-13}\mu_B$, where μ_B is the Bohr magneton. This magnetic moment is below the best astrophysical upper bounds for neutrino magnetic moments established in ref. [35]. We assume that neutrinos do not have transition magnetic moments, i.e. we study spin oscillations within one neutrino flavor, e.g., for electron neutrinos.

Neutrinos interact with background matter within the standard model. The effective potential is given in eq. (4.1). We suppose that the disk consists of the electroneutral hydrogen plasma. In this case, the effective potential in eq. (4.1) depends on the electron number density only. The maximal density in the disk is taken as $n_e^{(\max)} = 10^{18} \text{ cm}^{-3}$. Such a value is consistent with the observations carried out in ref. [36] for SMBH with $M = 10^8 M_\odot$.

The matter density and velocity depend on r and θ in the Polish doughnut model for the accretion disk. The typical density distribution is shown in figure 3 for different spins of BH. The accretion disk model has a free parameter K [see eq. (A.4)]. We vary K to make $n_e^{(\max)} = 10^{18} \text{ cm}^{-3}$ for all spins of BH.

The toroidal magnetic field has the same configuration in our calculations [see eqs. (4.3) or (A.2)]. We vary the parameter K_m in eq. (A.4) to reach $|\mathbf{B}|_{\max}^{(\text{tor})} = 320 \text{ G}$. This magnetic field strength is $|\mathbf{B}|_{\max}^{(\text{tor})} \sim 10^{-2} B_{\text{Edd}}$, where

$$B_{\text{Edd}} = 10^4 \text{ G} \times \left(\frac{M}{10^9 M_\odot} \right)^{-1/2}, \quad (5.1)$$

is the Eddington limit for the magnetic field in the vicinity of BH [37], which is $B_{\text{Edd}} \approx 3.2 \times 10^4 \text{ G}$ for $M = 10^8 M_\odot$.

We consider two models of the poloidal magnetic field in the disk. First, the vector potential is in eq. (A.7) [see also eq. (4.4)]. Second, A_μ is given eq. (A.8) [see also eq. (4.5)]. In the latter case, we choose the parameter b so that $|\mathbf{B}|_{\max}^{(\text{pol})} = 320 \text{ G}$. It means that the toroidal and poloidal fields have comparable strengths.

The initial flux of neutrinos is emitted from the point $(r_s, \theta_s, \phi_s) = (\infty, \pi/2, 0)$. All incoming neutrinos are left polarized. First, we reconstruct the neutrino trajectory, namely, the dependence $\theta(x)$ using eq. (2.3). Then, we use the $\theta(x)$ -dependence in eqs. (4.2)-(4.5), which converts eq. (3.5) into the ordinary differential equation. Finally, we integrate eq. (3.5) with $\mathbf{\Omega}_x$ in eq. (3.6) along each neutrino trajectory using the two-step Adams–Bashforth developed in ref. [17]. We deal with $\sim 2.5 \times 10^3$ test particles in each run.

6 Results

In this section, we present the results of numerical simulations with the parameters given in section 5.

We mention in section 1 that active neutrinos are left-polarized, i.e. their spin is opposite to the particle momentum. If the neutrino spin precesses in an external field, a particle becomes sterile, i.e. we will observe the effective reduction of the neutrino flux. If we define the survival probability P_{LL} , i.e. the probability to remain left-handed after scattering, the observed neutrino flux is $F_\nu = P_{\text{LL}} F_0$, where F_0 is the flux of ‘scalar’ particles, i.e. particles which propagate along geodesics lines without necessity to track their polarization. Hence, F_0 is the observed flux at no spin oscillations. The detailed study of F_0 was carried out in ref. [31]. Our main goal is to obtain F_ν/F_0 and examine its dependence on the parameters of the system.

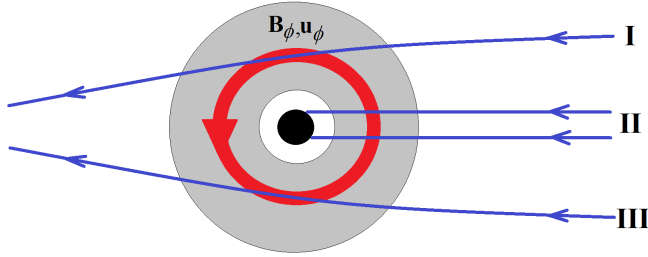


Figure 1. Schematic illustration of the neutrino interaction with a magnetized Polish doughnut, shown with gray color. The toroidal magnetic field and plasma velocity are concentrated mainly within the thin red torus. Neutrino trajectories, depicted with blue color, are separated into three regions. Regions I and III contain particles which interact with the longitudinal magnetic field. Neutrinos in region II interact with the transverse field, but they mainly fall to BH, shown with a black blob.

First, we mention that, in the scattering of ultrarelativistic neutrinos, the gravitational interaction only does not result in the neutrino spin-flip. This result was obtained in ref. [38] in the situation of a weak gravitational lensing. This fact was confirmed in refs. [16–18] for a strong gravitational lensing of neutrinos. Since our current simulations reveal the same feature, we omit the corresponding plot for F_ν/F_0 , which is trivial.

The toroidal magnetic field is inherent in a Polish doughnut accretion disk. The impact of the toroidal magnetic field on neutrino spin oscillations turns out to be negligible. The process of neutrino scattering and spin oscillations in a toroidal field is schematically depicted in figure 1. As seen in figure 3, the toroidal magnetic field is concentrated in a relatively thin torus. Spin oscillations are efficient if there is a significant transverse component of a magnetic field. In figure 1, one can see that particles in regions I and III in the incoming flux will interact mainly with a longitudinal magnetic field in their scattering. Despite particles in the region II interact with a transverse field, they are mainly within the shadow of BH. Hence, such neutrinos fall into BH and will not contribute to the observed flux. That is why the toroidal field with a reasonable strength does not modify the picture of spin oscillations.

If we consider the neutrino interaction with matter in the combination with the toroidal field, such external fields do not result in a significant spin oscillation. Indeed, it was found in ref. [7] that the interaction with matter only does not cause spin oscillations. It can only shift the resonance point. Thus, we omit the plots showing F_ν/F_0 for the case of the toroidal field and background matter.

The ratio of fluxes for neutrino gravitational scattering and the interaction with matter under the influence of both toroidal and poloidal field is shown in figure 2. We depict F_ν/F_0 for different spins of BH and various models of a poloidal field. The neutrino fluxes are given versus $\theta_{\text{obs}} = \theta(t \rightarrow +\infty)$ and $\phi_{\text{obs}} = \phi(t \rightarrow +\infty)$, which are angular coordinates of an outgoing neutrino. First, we note that the plots in figure 2 are symmetric with respect to the equatorial plane. It is the consequence of the fact that the flux of incoming neutrinos is parallel to the equatorial plane (see also appendix B).

Since the incoming neutrinos are emitted from the point $\theta_s = \pi/2$ and $\phi_s = 0$, the image of BH is mainly in the point $\theta_{\text{obs}} \approx \pi/2$ and $\phi_{\text{obs}} \approx \pi$. This feature is seen, especially, in figures 2(a) and 2(b), which correspond to an almost nonrotating BH. Despite figures 2(a) and 2(b) correspond to an almost Schwarzschild BH, these plots are not fully symmetric with respect to the vertical line $\phi_{\text{obs}} = \pi$. It happens since neutrinos interact with the rotating

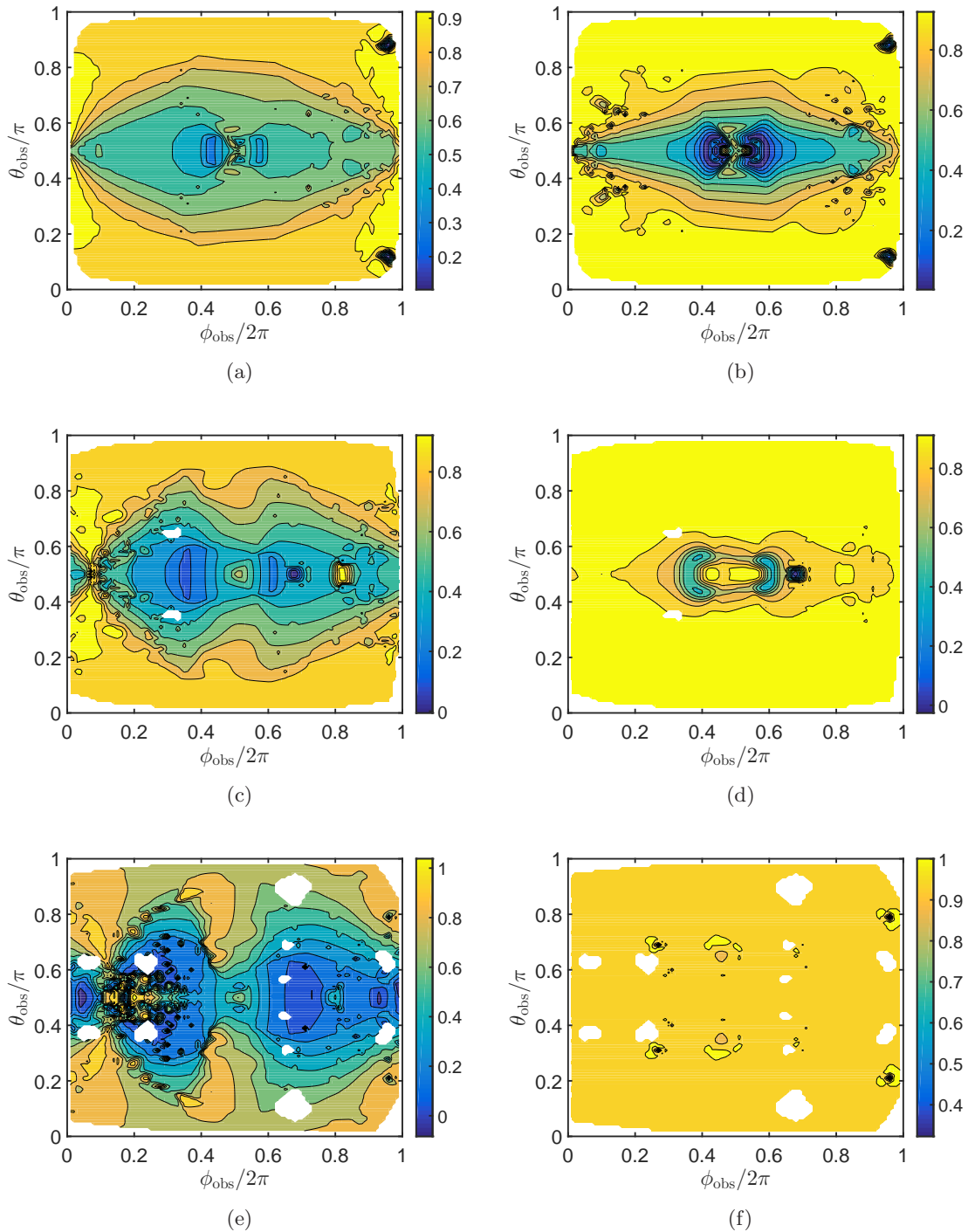


Figure 2. The observed neutrino flux normalized by F_0 for neutrinos scattered off a rotating SMBH with $M = 10^8 M_\odot$. The maximal number density in the disk is 10^{18} cm^{-3} . The maximal strengths of toroidal and poloidal fields are 320 G. The neutrino magnetic moment is $10^{-13} \mu_B$. Panels (a) and (b): $a = 2 \times 10^{-2} M$ ($z = 10^{-2}$); panels (c) and (d): $a = 0.5 M$ ($z = 0.25$); panels (e) and (f): $a = 0.9 M$ ($z = 0.45$). Panels (a), (c), and (e) correspond to the poloidal field in eq. (A.7); panels (b), (d), and (f) – in eq. (A.8). The rest of the parameters is the same as in figure 3.

accretion disk, where plasma moves with relativistic velocities. Again, referring to schematic plot in figure 1, it means that particles in regions I and III have different diagonal elements in the effective Hamiltonian \hat{H}_x since the velocities of plasma and neutrinos are in the same (region I) and the opposite (region III) directions.

If we compare figures 2(a), 2(c), and 2(e) with figures 2(b), 2(d), and 2(f), we can see that spin oscillations for the poloidal field in eq. (A.7) are more intense than for eq. (A.8). For example, spin oscillations are almost absent in figure 2(f). This feature is explained by the fact that the poloidal field in eq. (A.8) has a significant strength only in a small volume in the vicinity of BH (see, e.g., figure 4), whereas the field in eq. (A.7) slowly decreases towards the outer edge of the disk.

One can also see in figure 2 that there is a strong dependence of F_ν/F_0 on the spin of BH, especially for the poloidal field in eq. (A.8). It happens since the greater a is, the closer $|\mathbf{B}|_{\max}^{(\text{pol})}$ to the inner radius of the accretion disk is; cf. figure 4.

There are small white areas in figure 2 which increase with a . They appear because the 2D interpolation cannot correctly process plots with local insufficient number of points. This shortcoming can be eliminated by a significant enhancement of the test particles number.

7 Conclusion

We have studied neutrino scattering off a rotating SMBH surrounded by a thick magnetized accretion disk. Neutrinos were supposed to interact with BH gravitationally, as well as with matter of the disk electroweakly. The nonzero magnetic moment of Dirac neutrinos also allowed them to interact with the magnetic field in the disk. The interaction with external fields resulted in the precession of the neutrino spin which, in its turn, led to the effective reduction of the observed neutrino flux.

Our main goal was to find the observed neutrino flux accounting for spin oscillations, F_ν . It is shown in figure 2 for different spins of BH and various configurations of magnetic fields in the disk. We normalize F_ν to F_0 , which is the flux of scalar particles, i.e. at no spin oscillations.

In the present work, we have used the model of the accretion disk called the magnetized Polish doughnut [20]. This model predicts the self-consistent distributions of the matter density, angular velocity, and the toroidal magnetic field in the disk. Hence, our present results are the advance compared to the calculations in refs. [16–18] where the characteristics of accretion disks were taken from different sources.

Analogously to [16–18], here, we have confirmed that only gravitational interaction does not cause the spin-flip of ultrarelativistic neutrinos in their gravitational scattering. This fact is valid in a wide range of spins of BH. Thus, the only source of neutrino spin oscillations is the neutrino interaction with the magnetic field. We recall that the interaction with matter in case of ultrarelativistic neutrinos does not cause a spin-flip either. Moreover, we have found that the toroidal magnetic field within the magnetized Polish doughnut does not result in a significant change of the observed neutrino flux. It is the consequence of the quite compact location of the toroidal field.

A configuration with the only toroidal component is known to be unstable. That is why we have assumed that a poloidal magnetic field is present in the disk. We have considered two models of the poloidal field; cf. eqs. (A.7) and (A.8). The typical strengths of toroidal and poloidal fields were taken to be equal.

It should be noted that the presence of a strong poloidal magnetic field in an accretion disk around SMBHs is required in ref. [39] for the formation of jets from these objects. A nonzero poloidal component in an accretion disk was obtained using the MHD simulations in curved spacetime in ref. [40]. The analytical estimates for the relation between B_r and B_z components of the poloidal field can be also derived (see, e.g., ref. [41]).

Large scale magnetic fields in a thin accretion disk were studied in ref. [42]. However, a significant neutrino spin-flip is unlikely to be caused by external fields in a thin accretion disk since the neutrino path inside such a disk is quite short.

Our results in figure 2 show that spin effects are more sizable for the poloidal field in eq. (A.7). We have also revealed the dependence of the observed fluxes on the spin of BH. For example, one can see in figure 2(f) that the observed flux is almost unchanged for a rapidly rotating SMBH with the poloidal field in eq. (A.8).

It should be noted that, in our simulations, we have used quite moderate strengths of magnetic fields, as well as the matter density which is observed near some SMBHs [36]. The neutrino magnetic moment was taken to be below the current astrophysical upper bound [35]. It makes our results quite plausible.

Comparing figure 2 and figure 3, as well as figure 4, we can see that neutrino spin oscillations are the effective tool for the tomography of the distribution of the magnetic field in the vicinity of BH. The structure of a magnetic field, observed with help of neutrinos, is seen especially clearly for a relatively slowly rotating BH; cf. figures 2(a) and 2(b). Moreover, if one compares the fluxes in points, which are symmetric with respect to line $\phi_{\text{obs}} = \pi$, we can extract the information about the accretion disk rotation.

Our results can be useful for the exploration of external fields in the vicinity of BHs with help of neutrinos using existing or future neutrino telescopes [43, 44]. The penetrating power of neutrinos is much higher than that of photons. Perhaps, in future, neutrino telescopes will make a serious competition with the facilities like the Event Horizon Telescope in the studies of BHs vicinities.

We can apply our results to constrain the quantity μB_0 for neutrinos from a core-collapsing SN, which is expected in our galaxy [45]. Here, we rely on the poloidal magnetic field model in eq. (A.7) for the definitiveness. The predicted $F_{\text{pred}}(\theta_{\text{obs}}, \phi_{\text{obs}})$ and observed $F_{\text{obs}}(\theta_{\text{obs}}, \phi_{\text{obs}})$ neutrino fluxes in a certain direction $(\theta_{\text{obs}}, \phi_{\text{obs}})$ are related by $F_{\text{obs}} = P_{\text{LL}} F_{\text{pred}}$, where $P_{\text{LL}}(\theta_{\text{obs}}, \phi_{\text{obs}} | \mu B_0)$ is the survival probability shown in figure 2. Using the constraint on the magnetic field in the vicinity of SMBH in Sgr A*, $B < 10^2$ G, obtained in ref. [46], as well as figure 2, the upper bound on μ can be derived. However, it requires F_{obs} which will be available only after the observation of SN neutrinos.

A Magnetized Polish doughnut accounting for the poloidal magnetic field

In this appendix, we review the main properties of a magnetized Polish doughnut. The very detailed description of this model is given in ref. [20]. That is why we represent only the major expressions since the signature of our metric is mainly $(+, -, -, -)$, which is different from ref. [20].

All parameters of the disk depend on r and θ owing to the axial symmetry of the metric in eq. (2.1). The electromagnetic field tensor has the form,

$$F_{\mu\nu} = E_{\mu\nu\alpha\beta} U_f^\alpha B^\beta, \quad (\text{A.1})$$

where $E^{\mu\nu\alpha\beta} = \frac{\varepsilon^{\mu\nu\alpha\beta}}{\sqrt{-g}}$ is the antisymmetric tensor in curved spacetime with $\varepsilon^{tr\theta\phi} = 1$. The four vectors of the fluid velocity in the disk and the toroidal magnetic field are $U_f^\mu = (U_f^t, 0, 0, U_f^\phi)$ and $B^\mu = (B^t, 0, 0, B^\phi)$. We assume that the specific angular momentum of a particle in the disk $l = L/E$ is constant, $l = l_0$. It allows one to find the components of U_f^μ and B^μ ,

$$\begin{aligned} U_f^t &= \sqrt{\left| \frac{\mathcal{A}}{\mathcal{L}} \right|} \frac{1}{1 - l_0 \Omega}, & U_f^\phi &= \Omega U_f^t, \\ B^\phi &= \sqrt{\frac{2p_m^{(\text{tor})}}{|\mathcal{A}|}}, & B^t &= l_0 B^\phi, \end{aligned} \quad (\text{A.2})$$

where $\mathcal{L} = g_{tt}g_{\phi\phi} - g_{t\phi}^2$, $\mathcal{A} = g_{\phi\phi} + 2l_0g_{t\phi} + l_0^2g_{tt}$, and

$$\Omega = -\frac{g_{t\phi} + l_0g_{tt}}{g_{\phi\phi} + l_0g_{t\phi}}, \quad (\text{A.3})$$

is the angular velocity in the disk.

The disk density ρ and the magnetic pressure $p_m^{(\text{tor})}$ have the form,

$$\rho = \left[\frac{\kappa - 1}{\kappa} \frac{W_{\text{in}} - W}{K + K_m \mathcal{L}^{\kappa-1}} \right]^{\frac{1}{\kappa-1}}, \quad p_m^{(\text{tor})} = K_m \mathcal{L}^{\kappa-1} \left[\frac{\kappa - 1}{\kappa} \frac{W_{\text{in}} - W}{K + K_m \mathcal{L}^{\kappa-1}} \right]^{\frac{\kappa}{\kappa-1}}, \quad (\text{A.4})$$

where K , K_m , and κ are the constants in the equations of state, $p = Kw^\kappa$ and $p_m^{(\text{tor})} = K_m \mathcal{L}^{\kappa-1} w^\kappa$. Here, p is the plasma pressure and w is the specific enthalpy. Following ref. [20], we take that $\kappa = 4/3$. The form of the disk depends on the potential W ,

$$W(r, \theta) = \frac{1}{2} \ln \left| \frac{\mathcal{L}}{\mathcal{A}} \right|. \quad (\text{A.5})$$

The parameter W_{in} in eq. (A.4) is the value of W at the border of the disk.

Equations (A.2)-(A.5) completely define all the characteristics of the disk. First, using eq. (A.5), we get that points (r, θ) inside the disk obey the condition $W \leq W_{\text{in}}$. Then, we apply eq. (A.4) to find ρ and $p_m^{(\text{tor})}$. We define the effective toroidal field $|\mathbf{B}|^{(\text{tor})} = \sqrt{2p_m^{(\text{tor})}}$. The maximal value of $|\mathbf{B}|^{(\text{tor})}$ is equated to the strength expected in the disk. It gives us one of the equations to define the constants K and K_m . Another equation appears if we associate ρ_{max} with maximal plasma density present in the disk. Finally, eq. (A.2) gives us the rest of the parameters.

The distributions of the normalized electron number density $n_e/10^{18} \text{ cm}^{-3}$, where $n_e = \rho/m_p$, and the effective toroidal magnetic field $|\mathbf{B}|^{(\text{tor})} = \sqrt{2p_m^{(\text{tor})}}$, measured in Gauss, are shown in figure 3. for different spins of BH. We use the dimensionless variables $\tilde{K} = r_g^{4(1-\kappa)} K$ and $\tilde{K}_m = r_g^{2(1-\kappa)} K_m$. In all cases in figure 3, $n_e^{(\text{max})} = 10^{18} \text{ cm}^{-3}$ and $|\mathbf{B}|_{\text{max}}^{(\text{tor})} = 320 \text{ G}$. Figure 3 corresponds to $W_{\text{in}} = -10^{-5}$ and $\lambda_0 = 0.6(\lambda_{\text{mb}} + \lambda_{\text{ms}})$, where $\lambda_{\text{mb,ms}} = \lambda(x_{\text{mb,ms}})$ and

$$\lambda(x) = \frac{x^2 - z\sqrt{2x} + z^2}{\sqrt{2x^{3/2}} - \sqrt{2x} + z}. \quad (\text{A.6})$$

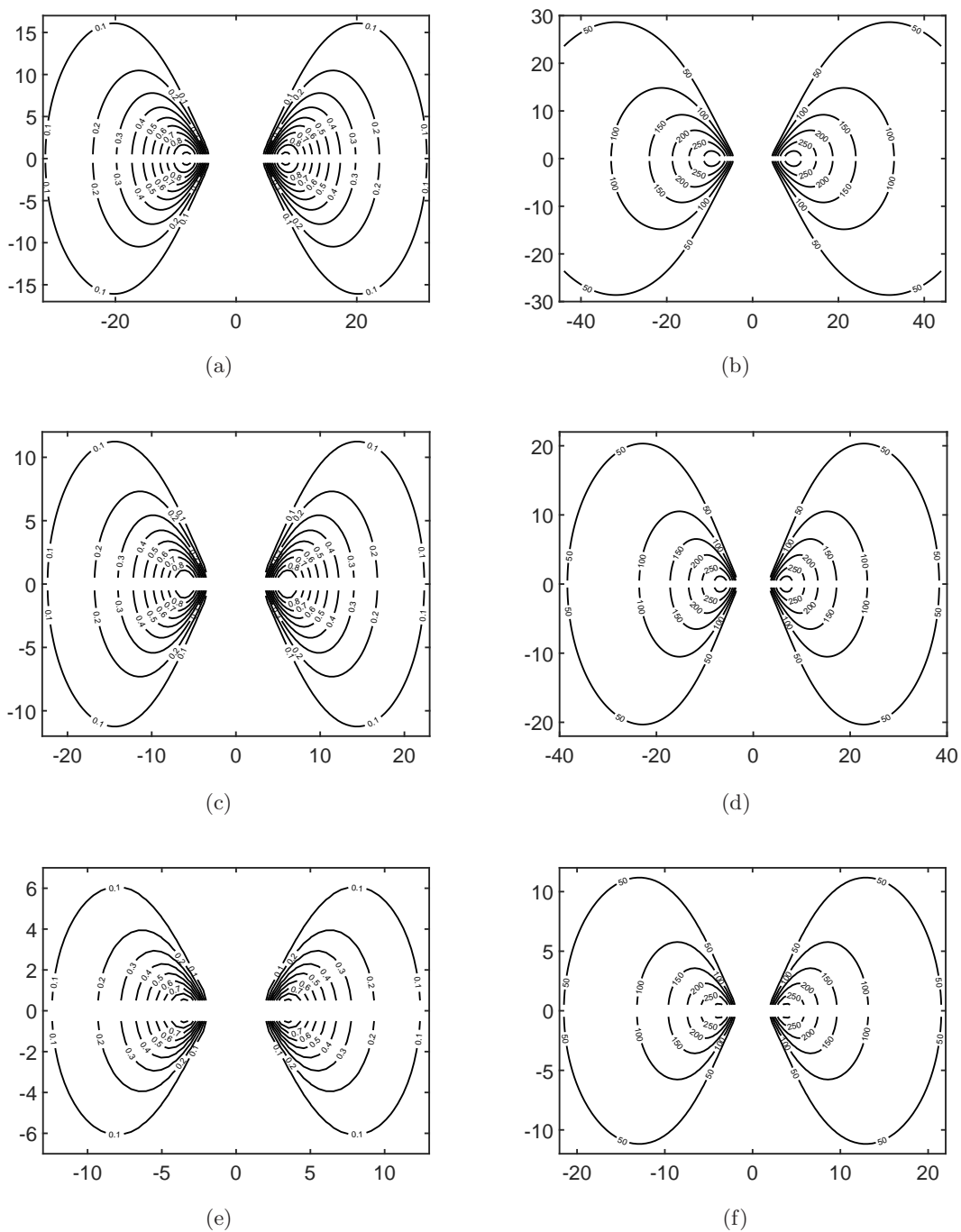


Figure 3. The distributions of the normalized electron number density $n_e/10^{18} \text{ cm}^{-3}$ [panels (a), (c), and (e)] and the effective toroidal magnetic field $|\mathbf{B}|^{(\text{tor})} = \sqrt{2p_m^{(\text{tor})}}$, in Gauss, [panels (b), (d), and (f)] for different spins of BH. Panels (a) and (b): $a = 2 \times 10^{-2}M$ ($z = 10^{-2}$), $\tilde{K} = 2.55 \times 10^{-31}$, and $\tilde{K}_m = 3.59 \times 10^{-41}$; panels (c) and (d): $a = 0.5M$ ($z = 0.25$) $\tilde{K} = 3.6 \times 10^{-31}$, and $\tilde{K}_m = 4.66 \times 10^{-41}$; panels (e) and (f): $a = 0.9M$ ($z = 0.45$) $\tilde{K} = 6.5 \times 10^{-31}$, and $\tilde{K}_m = 7.2 \times 10^{-41}$. The distances in the horizontal and vertical axes are in r_g .

That is, we study the disk corotating with BH. The quantities x_{mb} and x_{ms} are the radii of the marginally bound and marginally stable Keplerian orbits [47].

The model in ref. [20] provides only the toroidal magnetic field. It was proved in refs. [48, 49] that only a toroidal or only a poloidal magnetic field are unstable. The superposition of the these fields can be stable since it has a nonzero linking number and, thus, a nonzero magnetic helicity. That is why we suppose that a nonzero poloidal field is present in the disk. We consider two models for such a field.

First, we take the following vector potential:

$$A_t = Ba \left[1 - \frac{rr_g}{2\Sigma}(1 + \cos^2 \theta) \right], \quad A_\phi = -\frac{B}{2} \left[r^2 + a^2 - \frac{a^2 rr_g}{\Sigma}(1 + \cos^2 \theta) \right] \sin^2 \theta, \quad (\text{A.7})$$

where Σ is given in eq. (2.2). For the first time, A_μ in eq. (A.7) was proposed in ref. [50] to describe the electromagnetic field in the vicinity of a rotating BH which asymptotically equals to a constant and uniform magnetic field $\mathbf{B} = B\mathbf{e}_z$. Analogous magnetic field configuration is used, e.g., in ref. [51] to explain the cosmic rays acceleration by BH.

The assumption of the constant B in eq. (A.7) is unphysical since the magnetic field should vanish towards the outer edge of the disk. That is, following ref. [34], we assume that $B \propto B_0 r^{-5/4}$. The strength B_0 at $r \sim r_g$ is chosen to be close to $|\mathbf{B}|_{\text{max}}^{(\text{tor})}$. Previously, such a model of the poloidal field was used in refs. [16–18] in the whole space outside BH. Now, we suppose that it exists only inside the disk given by the condition $W \leq W_{\text{in}}$.

Second, we use the poloidal field, proposed in ref. [21],

$$A_\phi = b\rho, \quad (\text{A.8})$$

where b is a constant parameter and ρ in given in eq. (A.4). It should be noted that the poloidal field, corresponding to eq. (A.8), exists only inside the disk defined by $W \leq W_{\text{in}}$.

The only nonzero components of $F_{\mu\nu}$, corresponding to eq. (A.8), are $F_{r\phi} = b\partial_r \rho$ and $F_{\theta\phi} = b\partial_\theta \rho$. Using eq. (A.1), we find the magnetic pressure $p_m^{(\text{pol})} = -g_{\mu\nu} B^\mu B^\nu / 2$,

$$p_m^{(\text{pol})} = \frac{b^2}{2 \sin^2 \theta \Sigma} \left| \frac{\mathcal{L}}{\mathcal{A}} \right| \left[\frac{1}{\Delta} (\partial_\theta \rho)^2 + (\partial_r \rho)^2 \right], \quad (\text{A.9})$$

where Δ is given in eq. (2.2). We introduce the effective poloidal magnetic field $|\mathbf{B}|^{(\text{pol})} = \sqrt{2p_m^{(\text{pol})}}$. The parameter b in eq. (A.8) is fixed when we suppose that the maximal value of $|\mathbf{B}|^{(\text{pol})}$ equals to $|\mathbf{B}|_{\text{max}}^{(\text{tor})}$, which is defined earlier.

We show the distribution of $|\mathbf{B}|^{(\text{pol})}$ for eq. (A.9) for different spins of BH in figure 4. We present the situations when $z = 10^{-2}$ and $z = 0.5$. In the case of a rapidly rotating BH with $z = 0.9$, $|\mathbf{B}|^{(\text{pol})}$ has a very sharp maximum, which is hardly visible in a contour plot. Therefore, we omit it.

B Solution of the Schrödinger equation for neutrinos below the equatorial plane

In our problem, the flux of incoming neutrinos is both above and below the equatorial plane. We solve eq. (3.5) only for up particles. The solution for down particles can be reconstructed automatically applying the symmetry reasons.

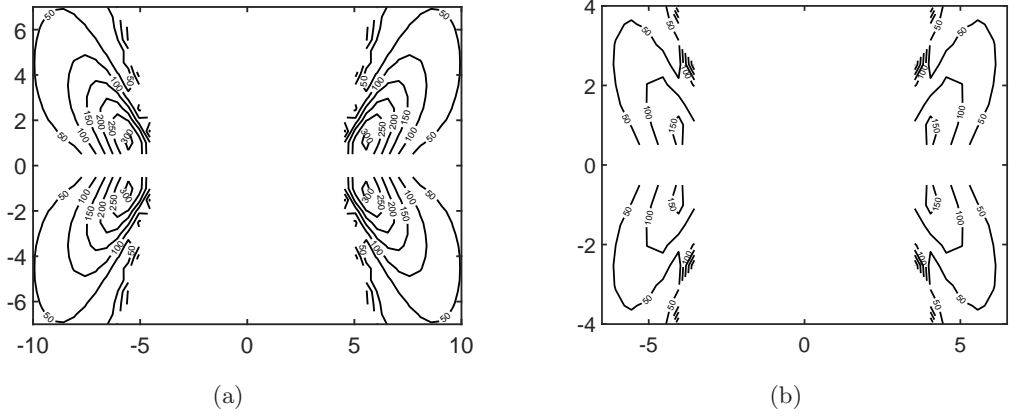


Figure 4. The distribution of the effective poloidal magnetic field $|\mathbf{B}|^{(\text{pol})} = \sqrt{2p_m^{(\text{pol})}}$, in Gauss, corresponding to eq. (A.8), for different spins of BH. Panel (a): $a = 2 \times 10^{-2}M$ ($z = 10^{-2}$) and $\tilde{b} = 6.42 \times 10^{-48}$; panel (b): $a = 0.5M$ ($z = 0.25$) and $\tilde{b} = 1.78 \times 10^{-48}$. The rest of the parameters is the same as in figure 3.

Suppose that the effective Hamiltonian in eq. (3.5) for up particles is \hat{H}_u . The Hamiltonian for down particles is $\hat{H}_d = -\hat{H}_u^*$, where the star means the complex conjugation. The formal solution of eq. (3.5) is

$$\psi_u(x) = \left[1 - i \int_{-\infty}^x \hat{H}_u(x') dx' - \frac{1}{2} \int_{-\infty}^x \hat{H}_u(x') dx' \int_{-\infty}^{x'} \hat{H}_u(x'') dx'' + \dots \right] \psi_{-\infty}, \quad (\text{B.1})$$

where $\psi_{-\infty}^T = (1, 0)$ is the initial condition. Taking the complex conjugation of eq. (B.1), we get

$$\begin{aligned} \psi_u^*(x) &= \left[1 + i \int_{-\infty}^x \hat{H}_u^*(x') dx' - \frac{1}{2} \int_{-\infty}^x \hat{H}_u^*(x') dx' \int_{-\infty}^{x'} \hat{H}_u^*(x'') dx'' + \dots \right] \psi_{-\infty} \\ &= \left[1 - i \int_{-\infty}^x \hat{H}_d(x') dx' - \frac{1}{2} \int_{-\infty}^x \hat{H}_d(x') dx' \int_{-\infty}^{x'} \hat{H}_d(x'') dx'' + \dots \right] \psi_{-\infty}. \end{aligned} \quad (\text{B.2})$$

Thus, $\psi_d(x) = \psi_u^*(x)$ since the initial condition is real and coincide for both particles.

Therefore $P_{\text{LL}}^{(u)} = |\psi_{+\infty}^{(u,L)}|^2 = P_{\text{LL}}^{(d)} = |\psi_{+\infty}^{(d,L)}|^2$. When we map the flux of outgoing down particles, we should take into account that $\phi_{\text{obs}}^{(d)} = \phi_{\text{obs}}^{(u)}$ and $\theta_{\text{obs}}^{(d)} = \pi - \theta_{\text{obs}}^{(u)}$.

References

- [1] SNO collaboration, Q.R. Ahmad et al., *Direct Evidence for Neutrino Flavor Transformation from Neutral- Current Interactions in the Sudbury Neutrino Observatory*, *Phys. Rev. Lett.* **89** (2002) 011301 [nucl-ex/0204008].
- [2] Super-Kamiokande collaboration, Y. Fukuda et al., *Evidence for Oscillation of Atmospheric Neutrinos*, *Phys. Rev. Lett.* **81** (1998) 1562 [hep-ex/9807003].
- [3] B.W. Lee and R.E. Shrock, *Natural suppression of symmetry violation in gauge theories: Muon- and electron-lepton-number nonconservation*, *Phys. Rev.* **D 16** (1977) 1444.

- [4] M. Dvornikov and A. Studenikin, *Electric charge and magnetic moment of a massive neutrino*, *Phys. Rev. D* **69** (2004) 073001 [hep-ph/0305206].
- [5] G.G. Raffelt, *Stars as Laboratories for Fundamental Physics: The Astrophysics of Neutrinos, Axions, and Other Weakly Interacting Particles*, University of Chicago Press, Chicago U.S.A. (1996), pgs. 304–309.
- [6] A.V. Kuznetsov, N.V. Mikheev and A.A. Okrugin, *Reexamination of a Bound on the Dirac Neutrino Magnetic Moment from the Supernova Neutrino Luminosity*, *Int. J. Mod. Phys. A* **24** (2009) 5977 [arXiv:0907.2905].
- [7] M.B. Voloshin, M.I. Vysotskiĭ and L.B. Okun', *Neutrino electrodynamics and possible consequences for solar neutrinos*, *Sov. Phys. JETP* **64** (1986) 446.
- [8] R. Wald, *Gravitational Spin Interaction*, *Phys. Rev. D* **6** (1972) 406.
- [9] A.A. Pomeranskiĭ and I.B. Khriplovich, *Equations of motion of spinning relativistic particle in external fields*, *J. Exp. Theor. Phys.* **86** (1998) 839. [gr-qc/9710098].
- [10] Y.N. Obukhov, A.J. Silenko and O.V. Teryaev, *General treatment of quantum and classical spinning particles in external fields*, *Phys. Rev. D* **96** (2017) 105005 [arXiv:1708.05601].
- [11] M. Dvornikov, *Neutrino spin oscillations in gravitational fields*, *Int. J. Mod. Phys. D* **15** (2006) 1017. [hep-ph/0601095].
- [12] S.A. Alavi and S. Nodeh, *Neutrino spin oscillations in gravitational fields in noncommutative spaces*, *Phys. Scr.* **90** (2015) 035301 [arXiv:1301.5977].
- [13] S. Chakraborty, *Aspects of Neutrino Oscillation in Alternative Gravity Theories*, *JCAP* **10** (2015) 019 [arXiv:1506.02647].
- [14] L. Mastrototaro and G. Lambiase, *Neutrino spin oscillations in conformally gravity coupling models and quintessence surrounding a black hole*, *Phys. Rev. D* **104** (2021) 024021 [arXiv:2106.07665].
- [15] R.C. Pantig, L. Mastrototaro, G. Lambiase and A. Övgün, *Shadow, lensing, quasinormal modes, greybody bounds and neutrino propagation by dyonic ModMax black holes*, *Eur. Phys. J. C* **82** (2022) 1155 [arXiv:2208.06664].
- [16] M. Dvornikov, *Gravitational scattering of spinning neutrinos by a rotating black hole with a slim magnetized accretion disk*, *Class. Quant. Grav.* **40** (2023) 015002 [arXiv:2206.00042].
- [17] M. Dvornikov, *Scattering of neutrinos by a rotating black hole accounting for the electroweak interaction with an accretion disk*, *Int. J. Mod. Phys. D* (2023) [arXiv:2212.03479].
- [18] M. Dvornikov, *Neutrino Spin and Flavor Oscillations in Gravitational Fields*, *Phys. Part. Nucl. Lett.* **20** (2023) 461 [arXiv:2304.03622].
- [19] M. Abramowicz, M. Jaroszynski and M. Sikora, *Relativistic, accreting disks*, *Astron. & Astrophys.* **63** (1978) 221.
- [20] S.S. Komissarov, *Magnetized tori around Kerr black holes: Analytic solutions with a toroidal magnetic field*, *Mon. Not. R. Astron. Soc.* **368** (2006) 993 [astro-ph/0601678].
- [21] P.Ch. Fragile and D.L. Meier, *General relativistic magnetohydrodynamic simulations of the hard state as a magnetically dominated accretion flow*, *Astrophys. J.* **693** (2009) 771 [arXiv:0810.1082].
- [22] M. Abramowicz and P.Ch. Fragile, *Foundations of Black Hole Accretion Disk Theory*, *Living Rev. Relativity* **16** (2013) 1 [arXiv:1104.5499].
- [23] Event Horizon Telescope collaboration, K. Akiyama et al., *First M87 event horizon telescope results. I. The shadow of the supermassive black hole*, *Astrophys. J. Lett.* **875** (2019) L1 [arXiv:1906.11238].

- [24] Event Horizon Telescope collaboration, K. Akiyama et al., *First Sagittarius A* Event Horizon Telescope Results. I. The Shadow of the Supermassive Black Hole in the Center of the Milky Way*, *Astrophys. J. Lett.* **930** (2022) L12.
- [25] V.S. Berezinsky and V.L. Ginzburg, *On high-energy neutrino radiation of quasars and active galactic nuclei*, *Mon. Not. R. Astron. Soc.* **194** (1981) 3.
- [26] R. Abbasi et al. (IceCube collaboration), *Search for neutrino emission from cores of active galactic nuclei*, *Phys. Rev.* **D 106** (2022) 022005.
- [27] P.J. Armitage and C.S. Reynolds, *The variability of accretion on to Schwarzschild black holes from turbulent magnetized discs*, *Mon. Not. R. Astron. Soc.* **341** (2003) 1041 [astro-ph/0302271].
- [28] O. Mena, I. Mocioiu and C. Quigg, *Gravitational Lensing of Supernova Neutrinos*, *Astropart. Phys.* **28** (2007) 348 [astro-ph/0610918].
- [29] S. Chandrasekhar, *The Mathematical Theory of Black Holes*, Clarendon, Oxford U.K. (1983).
- [30] S.E. Gralla, A. Lupsasca and A. Strominger, *Observational signature of high spin at the Event Horizon Telescope*, *Mon. Not. R. Astron. Soc.* **475** (2018) 3829 [arXiv:1710.11112].
- [31] M.Y. Grudich, *Classical gravitational scattering in the relativistic Kepler problem* (2014) [arXiv:1405.2919].
- [32] M. Dvornikov, *Neutrino spin oscillations in matter under the influence of gravitational and electromagnetic fields*, *JCAP* **06** (2013) 015 [arXiv:1306.2659].
- [33] M. Dvornikov and A. Studenikin, *Neutrino spin evolution in presence of general external fields*, *JHEP* **09** (2002) 016 [hep-ph/0202113].
- [34] R.D. Blandford and D.G. Payne, *Hydromagnetic flows from accretion discs and the production of radio jets*, *Mon. Not. Roy. Astron. Soc.* **199** (1982) 883.
- [35] N. Viaux, M. Catelan, P.B. Stetson, G.G. Raffelt, J. Redondo, A.A.R. Valcarce and A. Weiss, *Particle-physics constraints from the globular cluster M5: Neutrino Dipole Moments*, *Astron. & Astrophys.* **558** (2013) A12 [arXiv:1308.4627].
- [36] J. Jiang, A.C. Fabian, T. Dauser, L. Gallo, J.A. Garcia, E. Kara, M.L. Parker, J.A. Tomsick, D.J. Walton and C.S. Reynolds, *High Density Reflection Spectroscopy – II. The density of the inner black hole accretion disc in AGN*, *Mon. Not. R. Astron. Soc.* **489** (2019) 3436 [arXiv:1908.07272].
- [37] V.S. Beskin, *MHD Flows in Compact Astrophysical Objects: Accretion, Winds and Jets*, Springer, Heidelberg Germany (2010).
- [38] G. Lambiase, G. Papini, R. Punzi, and G. Scarpetta, *Neutrino Optics and Oscillations in Gravitational Fields*, *Phys. Rev.* **D 71** (2005) 073011 [gr-qc/0503027].
- [39] R.D. Blandford and R.L. Znajek, *Electromagnetic extraction of energy from Kerr black holes*, *Mon. Not. R. Astron. Soc.* **179** (1977) 433.
- [40] J.-P. De Villiers and J.F. Hawley, *A Numerical Method for General Relativistic Magnetohydrodynamics*, *Astrophys. J.* **589** (2003) 458 [astro-ph/0210518].
- [41] G.S. Bisnovatyi-Kogan and R.V.E. Lovelace, *Large Scale B-Field in Stationary Accretion Disks*, *Astrophys. J.* **667** (2007) L167 [arXiv:0708.2726].
- [42] X. Cao and H.C. Spruit, *The large scale magnetic fields of thin accretion disks*, *Astrophys. J.* **765** (2013) 149 [arXiv:1301.4543].
- [43] Hyper-Kamiokande collaboration, K. Abe et al., *Supernova Model Discrimination with Hyper-Kamiokande*, *Astrophys. J.* **916** (2021) 15 [arXiv:2101.05269].
- [44] JUNO collaboration, A. Abusleme et al., *JUNO Physics and Detector*, *Prog. Part. Nucl.*

- Phys.* **123** (2022) 103927 [arXiv:2104.02565].
- [45] K. Rozwadowska, F. Vissani and E. Cappellaro, *On the rate of core collapse supernovae in the Milky Way*, *New Astron.* **83** (2021) 101498 [arXiv:2009.03438].
- [46] R.P. Eatough et al., *A strong magnetic field around the supermassive black hole at the centre of the Galaxy*, *Nature* **501** (2013) 391 [arXiv:1308.3147].
- [47] J.M. Bardeen, W.H. Press and S.A. Teukolsky, *Rotating black holes: Locally nonrotating frames, energy extraction, and scalar synchrotron radiation*, *Astrophys. J.* **178** (1972) 347.
- [48] R.J. Tayler, *The Adiabatic Stability of Stars Containing Magnetic Fields–I: Toroidal Fields*, *Mon. Not. R. Astron. Soc.* **161** (1973) 365.
- [49] P. Markey and R.J. Tayler, *The Adiabatic Stability of Stars Containing Magnetic Fields–II: Poloidal Fields*, *Mon. Not. R. Astron. Soc.* **163** (1973) 77.
- [50] R.M. Wald, *Black hole in a uniform magnetic field*, *Phys. Rev. D* **10** (1974) 1680.
- [51] A.Yu. Neronov, D.V. Semikoz and I.I. Tkachev, *Ultra-High Energy Cosmic Ray production in the polar cap regions of black hole magnetospheres*, *New J. Phys.* **11** (2009) 065015 [arXiv:0712.1737].